sustainability

MDPI

Article

Research on Sensor Placement for Disaster Prevention in Water Distribution Networks for Important Users

Jiajia Wu [1], Donghui Ma [2,3], Wei Wang [2,3,*] and Zhao Han [1]

[1] College of Architecture and Civil Engineering, Beijing University of Technology, Beijing 100124, China; snail_s@emails.bjut.edu.cn (J.W.); hanzhao@emails.bjut.edu.cn (Z.H.)
[2] Institute of Earthquake Resistance and Disaster Reduction, Beijing University of Technology, Beijing 100124, China; mdh@bjut.edu.cn
[3] College of Architecture and Urban Planning, Beijing University of Technology, Beijing 100124, China
* Correspondence: ieeww@bjut.edu.cn; Tel.: +86-158-0162-8620

Received: 2 December 2019; Accepted: 13 January 2020; Published: 19 January 2020

check for updates

Abstract: Sensor placement for disaster prevention for important users in urban water distribution networks is essential for post-earthquake monitoring and repair. Herein, we proposed a sensor placement approach for disaster prevention monitoring for important users, to (a) improve the fault diagnosis ability of the water distribution network and to (b) guarantee the function of emergency services for key nodes after an earthquake. First, an evaluation system of node users' disaster prevention impact factors was presented to evaluate the node influence degree from three aspects: post-earthquake leakage, emergency support and topology structure; and the weight values of node users' disaster prevention impact factors were obtained. Second, a post-earthquake hydraulic analysis model based on the pressure-driven demand was used to calculate the water shortage ratio of nodes. Third, using the three-way clustering integration method, the results of four clustering techniques were integrated to divide the monitoring domain in the water distribution network based on sensitivity analysis. Finally, on basis of the sensitivity matrix, the division of the monitoring area and the impact factors of node users' disaster prevention were combined to place sensors for post-earthquake disaster prevention in the water distribution network. Detailed computational experiments for a real urban water network in China were performed and compared with the results of other traditional techniques to evaluate the performance of the proposed approach. The results show that the approach is better than traditional methods. It not only considers the actual hydraulic information of the water distribution network, but also the important user nodes after an earthquake, and is of great significance for emergency command and rescue and disaster relief after an earthquake in the city.

Keywords: water distribution network; sensor placement; node users' impact factors of disaster prevention; pressure-driven demand model; monitoring domain division

1. Introduction

As a key emergency infrastructure in the event of an earthquake, the urban water supply system is an important basic condition for earthquake relief and life safety guarantee [1]. As a part of the lifeline system, a water distribution network (WDN) not only plays a momentous role in the normal operation of the city, but is also particularly important for water use in earthquake shelters and the rescue of secondary disasters. However, WDNs often suffer from varying degrees of earthquake damage, resulting in loss or weakening of functions, which cannot meet the post-earthquake emergency rescue service function. If the key user nodes cannot be guaranteed to use water after an earthquake, this will have a negative impact on the rescue. Therefore, it is crucial to place sensors for disaster prevention considering important users for strengthening the efficiency of post-earthquake monitoring of WDNs, ensuring the water demand of important user nodes, and improving the emergency repair ability of the lifeline system after a disaster.

The protection and monitoring of important nodes or pipelines are important aspects of improving the resilience of the lifeline network. Jie Li et al. [2] introduced an element investment importance analysis in the seismic topology optimization research of the lifeline network, and analyzed the nodes and lines of high importance in the lifeline network in order to speed up the convergence of optimization processes. Considering node importance and power generation recovery capability, Can Zhang et al. [3] proposed a two-stage grid reconfiguration strategy, which involves a node importance evaluation method based on the concept of regret. Wenli Fan et al. [4] put forward a method for evaluating the importance of multi-attribute nodes in complex grids based on the Gini coefficient. They introduced the Gini coefficient, used in economics, to the importance evaluation of multi-attribute nodes as well as to determine the weights of indicators. Considering the node importance, Fei Wang et al. [5] proposed a classification of emergency repair scope for urban WDNs, and grouped them from three aspects using graph theory: node importance, function importance and structure importance. Anne-Marie Kermarrec et al. [6] introduced a novel form of centrality: the second order centrality, which can be used to accurately identify critical nodes as well as to globally characterize graphs' topology in a distributed way. Through the application of the neighborhood rule, Ahmad Zareie et al. [7] proposed an index to determine node centrality using the notions of Shannon entropy and Jensen–Shannnon divergence for ranking influential nodes. Michalis Fragiadakis et al. [8] presented a methodology for the seismic assessment of the reliability of urban WDNs based on general seismic assessment standards, which incorporates data of past non-seismic damage, the vulnerabilities of the network components against seismic loading, and the topology of an urban WDN. The above research works evaluated the importance of network nodes or lines in terms of network functions, topological structure and post-disaster reliability. If the importance assessment is introduced into the monitoring sensor placement study, the priority of protection and monitoring of important nodes or pipelines in the network analysis can be improved.

The research studies on sensor placement are currently concentrated in the field of health monitoring. It is the focus of the problem to study the optimal placement of sensor from the aspects of the monitoring domain and sensitivity based on monitoring parameters. The existing research works mostly use optimization algorithms and clustering algorithms to solve these two requirements, such as sensitivity analysis, neural network algorithms, genetic algorithms [9] and fuzzy clustering algorithms. Different clustering algorithms actually reflect the different levels of clustering parameters and different degrees of consideration. Lingli Chen [10] used the effective independence method (EfI), the Fisher information matrix (FIM) maximization criterion, and the correlation coefficients method to achieve optimal sensor placement. It was concluded that the calculation process of the node correlation coefficient method is relatively simple and stable, which increases the consideration of the parameters' difference in essence. D. Kowalski et al. [11] proposed a fractal geometry method for water quality and pressure monitoring systems in WDNs, which incorporates the impact of network structure and user characteristics into the analysis. Jonas Kjeld Kirstein et al. [12] used topological clustering as a tool for water supply utilities for monitoring preparation and contamination contingency plans. Using a pressure sensitivity matrix and an exhaustive search strategy, Fatiha Nejjarih et al. [13] presented an optimal sensor placement strategy. In their work, the evidence C-means clustering method was applied to reduce the scale and complexity of the placement problem, and the effectiveness of this strategy was demonstrated by an example of a WDN in Barcelona. Adria Soldevila et al. [14] proposed an approach for sensor placement in WDNs by using a classifier to locate leakage, which combines correlation and redundancy with a genetic algorithm by using a hybrid feature selection algorithm. These studies show the degree to which different methods consider the feature factors. In the research of disaster prevention monitoring layout, the introduction of the feature of important nodes that need to be protected and monitored after an earthquake can be used as the basic research idea of this paper.

In terms of post-earthquake hydraulic calculation, the University of Cornell has developed GIRAFFE software, which assumes that there are only two cases of node water demand after an earthquake in a WDN: fully supplied or completely not supplied [15–18]. In fact, WDN is in a low-pressure water supply state after an earthquake, and the nodes are partially supplied rather than fully supplied [19,20]. Zhao Han et al. [21] presented a post-earthquake hydraulic analysis model of WDN based on the pressure-driven demand (PDD), which overcomes the above shortcomings.

In addition, most clustering algorithms are unstable, and mostly depend on parameters and initialization to a great extent, which may produce different results for the same dataset [22,23]. Therefore, the clustering integration method has been proposed and widely considered, and it shows higher robustness and stability than single clustering algorithms. LingChao Hu [24] proposed a voting-based three-way decision clustering integration method, which is more robust than a single clustering method.

In this paper, we proposed a sensor placement strategy for disaster prevention for important users. Based on the hydraulic analysis, an evaluation system of node users' disaster prevention impact factors was established, and the impact factor weight values of node users were calculated from the three aspects of post-earthquake water shortage, emergency support and topological structure. The post-earthquake hydraulic analysis model based on PDD was used to calculate the water shortage ratio of nodes, which was combined with the consideration of the importance features as the placement optimization parameter. On this basis, using the three-way decision cluster integration method and integrating four clustering methods to divide the monitoring domain, the decision-making value of different clustering methods can be reflected comprehensively. The structure of this paper is displayed in Figure 1.

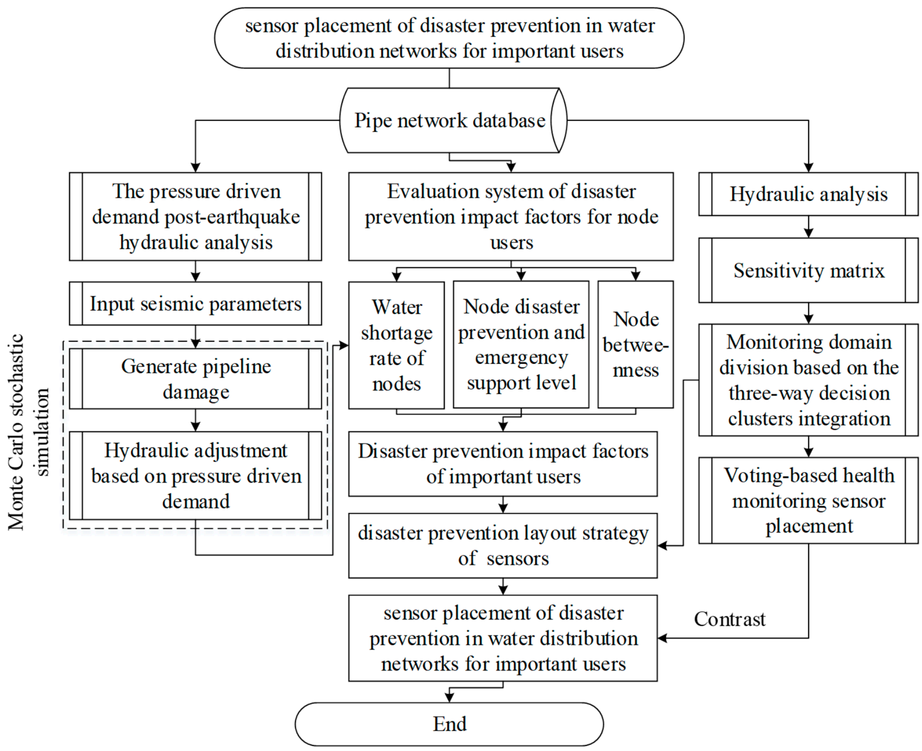

Figure 1. The structure of this paper.

2. Disaster Prevention Impact Factors of Node Users

Sensor placement for health monitoring considers the sensor's optimal placement during daily leakage. After an earthquake, the key node user of the WDN plays a decisive role in disaster relief and water use for victims. Therefore, for protecting people's lives, it is necessary to evaluate the important nodes of WDNs before earthquakes. Thus, we proposed an evaluation system of disaster prevention impact factors for important node users of WDNs. The nodal leakage can reflect the strength of the nodal water transport function after an earthquake. In addition, considering that the locations of the nodes belong to different levels of disaster prevention emergency support objects, such as municipal emergency command centers, fire control centers, special service fire stations, and central evacuation sites, we thought that the minimum guarantee levels of these emergency protection objects can directly reflect the important position and influence degree of the nodes in a WDN after an earthquake. In terms of topology, the betweenness of a node indicates the importance of the node in the network. Therefore, from three aspects: water shortage, earthquake emergency prevention and topology, the evaluation system for node users' impact factors in a WDN was constructed (Figure 2).

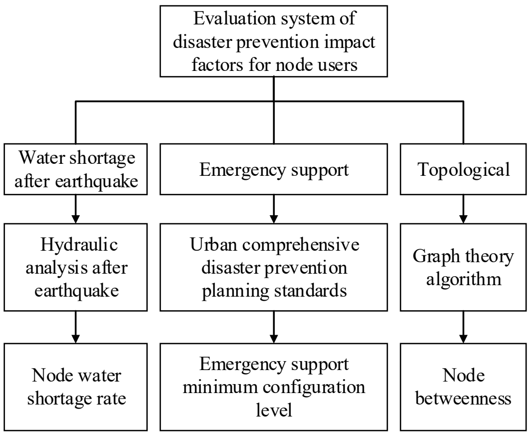

Figure 2. The evaluation system structure for disaster prevention impact factors of node users.

2.1. Node Water Shortage Calculation Based on PDD

The PDD post-earthquake hydraulic analysis model [21] assumes that the nodal water demand is supplied when the node water pressure reaches or exceeds the design water pressure. The node water supply is 0 when the node water pressure is lower than or equal to the minimum water pressure. The node water demand and node water pressure should meet a certain functional relationship, when the node water pressure is between the design water pressure and the minimum water pressure. The relationship between nodal water pressure and nodal water demand proposed by Wagner et al. [25] was adopted, as shown in Equation (1):

$$Q_i{}^* = \begin{cases} 0 & , \quad H_i < H_i^{\min} \\ Q_i \cdot \sqrt{\dfrac{H_i - H_i^{\min}}{H_i^{des} - H_i^{\min}}} & , \quad H_i^{\min} \le H_i < H_i^{des} \\ Q_i & , \quad H_i^{des} \le H_i \end{cases} \tag{1}$$

where $Q_i{}^*$ is the water supply of node i considering the relationship between node water pressure (m) and water demand (L/s), Q_i is the initial water demand of node i (L/s), H_i is the calculated water pressure of node i (m), $H_i{}^{min}$ is the minimum node water pressure required for node i water supply greater than 0 (m), and $H_i{}^{des}$ is the design water pressure required for node i to meet the initial water demand Q_i (m).

To determine the number and location of the damage points, we utilized Monte Carlo simulation to generate a series of random numbers of pipeline seismic damage that obey uniform distribution along the length of the pipeline. For each damage point, two damage states (break and leakage) were generated by a Monte Carlo simulation random process again to form the post-earthquake hydraulic model. Finally, epanet2.dll was used to calculate the hydraulic adjustment of WDN based on PDD. The calculations of the average repair rate, *RR*, pipeline leakage form and leakage area are based on the statistical data of pipeline damage in the Northridge earthquake [26]. The basic calculation flow of the PDD model is shown in Figure 3.

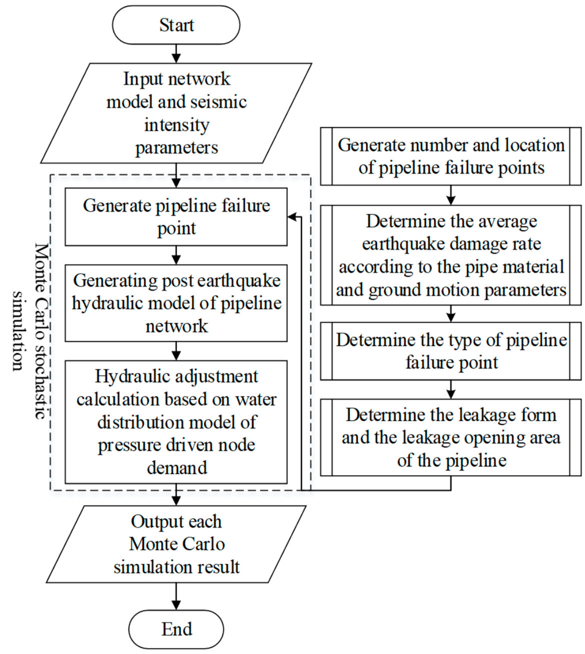

Figure 3. Post-earthquake hydraulic model based on pressure-driven demand in a water distribution network.

The nodal demand pressure was set to 20 m; after simulating n times, the simulation results of the required water pressure were selected when the post-earthquake water pressure of the node was lower than the normal state. Note that when the water pressure of all nodes meets the minimum required water pressure in the simulation, the water demand of the simulation is the same as the water demand under normal conditions, so the calculation of the water demand in this situation was neglected.

Calculate the average water demand of the nodes after an earthquake, see Equation (2):

$$\overline{Q_i} = \frac{1}{k}\sum_{j=1}^{k} Q_i^k \tag{2}$$

where $\overline{Q_i}$ is the average post-earthquake water demand of node i, and ${Q_i}^k$ is the water demand of the node I obtained by the k-th simulation. The post-earthquake water shortage rate of the node is calculated by Equation (3):

$$\Delta q_i = \frac{Q_i - \overline{Q_i}}{Q_i} \tag{3}$$

where Δq_i is the post-earthquake water shortage rate of node i, and Q_i is the water demand of node i under the normal condition. The greater the post-earthquake water shortage rate of the node, the greater the degree of influence of the node.

2.2. Emergency Support Level

The safety function guarantee level of an emergency support infrastructure, such as urban emergency traffic, water supply, power supply, communication, etc., specified in Article 6.1.2 of the "Urban Comprehensive Disaster Prevention Planning Standards" [27] in China is divided into I, II and III. The classification of emergency support level reflects the importance of urban emergency support objects after an earthquake. We associated the key emergency support objects of WDN with node users, which can reflect the post-earthquake significance of nodes. According to the emergency support objects corresponding to the nodes, the nodes' levels were determined, and the emergency support levels of the nodes were scored (Table 1).

Table 1. The corresponding score of emergency support levels of the nodes.

Level of Emergency Support	Score
I	4
II	3
III	2
—	1

2.3. Node Betweenness

A graph can be represented by Equation (4) [28]:

$$G(V, E) \tag{4}$$

where V is a non-empty vertex set, and E is the edge set.

A graph is uniquely determined by the association between its vertices and edges, and also by the adjacency between its vertices. The matrix $A = A(G) = (a_{ij})_{n\times n}$ is called the adjacency matrix of graph G, where a_{ij} is used to represent the number of edges between vertex v_i and vertex v_j, which may be 0,1.

According to the adjacency matrix of a graph, the betweenness of a graph can be calculated. The betweenness is divided into two types: node betweenness and edge betweenness. The minimum path between node i and node j in the network will pass through some nodes; if a node k is passed by many shortest paths, it means that the node k is very important in the network. The importance or influence of node k can be expressed by the node betweenness, which is defined as:

$$B_k = \sum_{i,j\in C} \frac{d(i,j)_k}{d(i,j)} \tag{5}$$

where B_k is the betweenness of node k, $d(i,j)$ is the shortest path numbers between node i and node j, and $d(i,j)_k$ is the minimum number of paths between node i and node j passing through node k.

2.4. Evaluation System of Disaster Prevention Impact Factors for Node Users

Factor index set $z = \{z_1, z_2, \ldots, z_k\}$, $k = \{1, 2, 3\}$ is selected, where z_1 is the node water shortage rate, z_2 is the earthquake disaster prevention emergency support level score, and z_3 is the node betweenness. The influence value $\left\{s_i^{z_k}\right\}$ under each factor indicator, indicating the influence value of node i under the factor indicator z_k, is calculated. According to the influence value, the relative influence matrix F^{z_k} of the node under the factor index z_k is calculated by the formula (6), which measures the relative influence of each node under one index.

$$F^{z_k} = \left\{ \begin{array}{cccc} f_{11}^{z_k} & f_{12}^{z_k} & \cdots & f_{1n}^{z_k} \\ f_{21}^{z_k} & f_{22}^{z_k} & \cdots & f_{2n}^{z_k} \\ \vdots & \vdots & \ddots & \vdots \\ f_{n1}^{z_k} & f_{n2}^{z_k} & \cdots & f_{nn}^{z_k} \end{array} \right\} \tag{6}$$

where $f_{ij}^{z_k}$ is the relative influence value of node i and node j under the factor indicator z_k, and n is the total number of nodes. When $i = j$, $f_{ij}^{z_k}$ has no practical meaning and takes a value of 0; when $i \neq j$, it is calculated by Equation (7):

$$f_{ij}^{z_k} = \begin{cases} 1 & s_i^{z_k}/s_j^{z_k} > 1 \\ 0.5 & s_i^{z_k}/s_j^{z_k} = 1 \\ 0 & s_i^{z_k}/s_j^{z_k} < 1 \end{cases} \tag{7}$$

In order to obtain the relative influence vector of the node under the factor index z_k, the row vector elements of the relative influence matrix F^{z_k} of the node are summed by Equation (8):

$$F^{z_k}(i) = \sum_{i=1}^{n} f_{ij}^{z_k} \tag{8}$$

The relative influence vector of the node only describes the relative influence of the node under one evaluation index. To synthesize the relative influence value of the node under different indicators, the node's comprehensive influence matrix F is constructed by using the relative influence vector of the node under different indicators (9):

$$F = \begin{Bmatrix} F_1^{z_1} & F_1^{z_2} & \cdots & F_1^{z_k} \\ F_2^{z_1} & F_2^{z_2} & \cdots & F_2^{z_k} \\ \vdots & \vdots & \ddots & \vdots \\ F_n^{z_1} & F_n^{z_2} & \cdots & F_n^{z_k} \end{Bmatrix} \tag{9}$$

The sum of each row of the node's comprehensive influence matrix F is summed to obtain the comprehensive relative influence values $F_1, F_2, \ldots, F_n$ of the nodes, which reflect the comprehensive relative influence of the nodes under different factors. Finally, the normalization method based on degree of membership is used to process the node's comprehensive relative influence values to obtain the node users' impact factor values.

The Gaussian membership function expression is:

$$\overline{F_i} = e^{\frac{(F_i - c)^2}{2\sigma^2}} \tag{10}$$

$$c = (1 + \varepsilon)F_{max} \tag{11}$$

$$\sigma = (0.5 + \varepsilon)Fmin_{max} \tag{12}$$

where $\overline{F_i}$ is the node i user's disaster prevention impact factor value of WDN, F_{max} is the maximum value of the comprehensive relative influence set $\{F_1, F_2, \ldots, F_n\}$, F_{min} is the minimum value of the integrated relative influence set $\{F_1, F_2, \ldots, F_n\}$, ε is the normalized parameter, and the value range is $\varepsilon \in (0, 1)$.

3. Calculation of Disaster Prevention Impact Factors for Node Users

3.1. Sensitivity Matrix

The pressure sensitivity of nodes reflects the influence of the pressure on other nodes when an abnormality occurs in one node. Assuming that there are n nodes in the WDN, the node pressure vector $\{P^0\}$ of WDN under the normal working condition is obtained by hydraulic analysis of EPANET software:

$$\left\{P^0\right\} = \left\{P_1^0, P_2^0, \cdots, P_n^0\right\}^T \tag{13}$$

where ${P_n}^0$ is the water pressure of the n-th node(m). Then, the initial matrix $[P^0]$ of node pressure is constructed by n-column $\{P^0\}$. Comparing the node pressure changes calculated by 10%, 30% and 50% of the minimum user flow, the leakage of the minimum user flow that makes the clustering effect the best is selected. After calculation, we took 50% of the minimum node user flow as the node leakage, and the node pressure matrix $[P]$ is:

$$[P] = \begin{bmatrix} P_{11} & P_{12} & \cdots & P_{1n} \\ P_{21} & P_{22} & \cdots & P_{2n} \\ \vdots & \vdots & \ddots & \vdots \\ P_{n1} & P_{n2} & \ldots & P_{nn} \end{bmatrix} \tag{14}$$

where P_{ij} is the pressure value of node i when the node j leaks.

The pressure sensitivity matrix $[\Delta P]$ is obtained by subtracting the node pressure matrix $[P]$ from the initial pressure matrix $[P^0]$ of the node pressure.

$$[\Delta P] = \left[P^0\right] - [P] \tag{15}$$

$$[\Delta P] = \begin{bmatrix} \Delta P_{11} & \Delta P_{12} & \cdots & \Delta P_{1n} \\ \Delta P_{21} & \Delta P_{22} & \cdots & \Delta P_{2n} \\ \vdots & \vdots & \ddots & \vdots \\ \Delta P_{n1} & \Delta P_{n2} & \cdots & \Delta P_{nn} \end{bmatrix} \tag{16}$$

where Δp_{ij} is the pressure change value of the node i when the node j leaks.

The sensitivity matrix of nodal pressure was obtained by dimensionless normalization based on the extremum method.

$$l_{ij} = \frac{\Delta p_{ij} - min(\Delta p)}{max(\Delta p) - min(\Delta p)} \tag{17}$$

The comprehensive sensitivity of the node is calculated from Equation (18):

$$L_i = \sqrt{\sum_{j=1}^{n} \left|l_{ij}\right|^2} \tag{18}$$

where L_i is the comprehensive sensitivity of node i. The comprehensive sensitivity of a node indicates the pressure sensitivity of the node to the flow change.

On the basis of clustering integration, according to the monitoring domain node classification, the intra-class normalization of the node comprehensive sensitivity is performed by Equation (19), which indicates the sensitivity of the node in the corresponding class.

$$\overline{L_i} = \frac{L_i - L_{min}}{Lmin_{max}, i \in C} \tag{19}$$

where C is the monitoring domain category, $\overline{L_i}$ is the comprehensive sensitivity of node i in class C after normalization, also called the intra-class sensitivity of node i, and L_{min} is the minimum comprehensive sensitivity in class C.

3.2. Strategy for Disaster Prevention Sensor Placement

The principle of the disaster prevention sensor placement is not only to ensure the pressure sensitivity of the monitoring nodes, but also to consider the needs of the post-earthquake disaster prevention function of the node users. The placement should be arranged on the important user nodes or the adjacent nodes as far as possible. Thus, we considered the principle of the disaster prevention sensor placement and proposed a layout strategy for disaster prevention monitoring points.

The node comprehensive sensitivity of each class of the monitoring domain and the corresponding impact factor weights can be obtained from Equations (19) and (10). Next, the appropriate threshold was selected to consider the degree of sensitivity at the monitoring point:

$$\overline{L_i} > \psi, i \in C \tag{20}$$

where ψ is the given threshold. Then, the weights of node disaster prevention impact factors corresponding to the node of Equation (20) are ranked from large to small, and the node corresponding to the maximum disaster prevention impact factor weight is selected as the node for installation of monitoring equipment.

It should be noted that the choice of threshold directly affects the sensor placement, so a suitable threshold could balance the sensitivity and the influence of the node. In actual calculations, the threshold should be adjusted in conjunction with the scale of the WDN.

4. Simulation and Comparison

Figure 4 shows a water distribution model based on actual data from a region in China [29], which has 53 nodes and 78 pipelines. Node 50 is a reservoir; node 51, node 52, and node 53 are water source nodes; and the total hydraulic heads are 76.95 m, 74.31 m, 83.58 m and 81.98 m, respectively. We assumed that pipes with a diameter greater than 600 mm are riveted steel pipes, while pipes with a diameter less than 600 mm are rubber sealed cast iron. It needs to be mentioned that all methods were based on Matlab software, and the hydraulic calculation was called epanet2.dll. For the basic data of the WDN, see [29]:

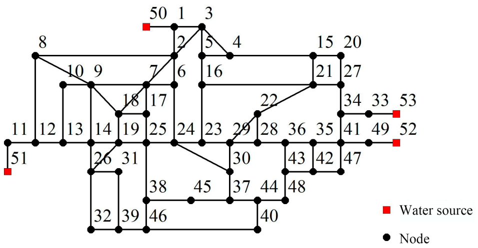

Figure 4. Water distribution network model.

Based on the hydraulic analysis, the nodal pressure sensitivity model was used to obtain the sensitivity matrix, and the extreme value processing method was used to normalize the node pressure sensitivity matrix. Xunjian Wang, Zengyi Wang [30] suggested that the setting of the WDN monitoring points should be about $\frac{1}{7} \sim \frac{1}{6}$ of the total number of nodes, and the number of monitoring points of a large pipe network is smaller than that of a small pipe network. Therefore, the ratio of the monitoring points number in this paper to the total number of nodes was selected as 1/7, that is, the number of monitoring points is 7.

4.1. Disaster Prevention Impact Factors of Node Users

4.1.1. Node Water Shortage Rate

According to the table of seismic intensity in China (GB/t 17742-2008) [31], we chose the peak ground velocity (*PGV*) of the IX seismic intensity to calculate the average repair rate, *RR*, in which the average repair rate of pipelines with diameter greater than 600 mm is 0.0690, and that of pipelines with diameter less than 600 mm is 0.1254. The PDD post-earthquake hydraulic analysis model was used to simulate a total of 25 times, and all nodes satisfied the water requirements in the sixth, 10th, 12th, 19th and 20th simulations. Therefore, when calculating the water shortage rate, we did not consider the results of the above five simulations. The remaining 20 simulation results of the node average shortage rate value are shown in Figure 5.

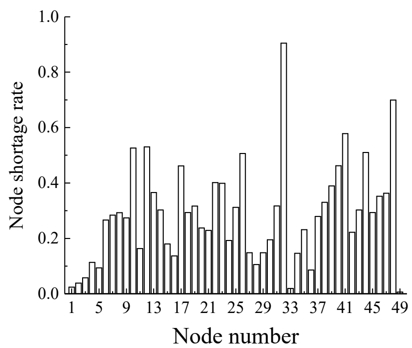

Figure 5. Node water shortage rate.

4.1.2. Node Emergency Support Rating

We assumed the emergency guarantee level of the node in this paper (Figure 6), and we analyzed the node user impact factor values of the WDN according to the node users' impact factor evaluation system proposed in the above section.

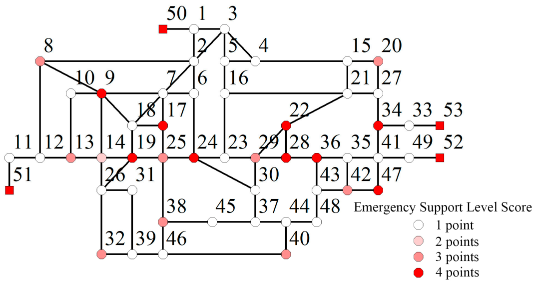

Figure 6. The score map of node emergency support level.

The nodes with an emergency protection level score of 3 or more are mainly concentrated in the eastern, northeastern, western and northwestern regions of the city (Figure 6). The monitoring sensors should be placed as much as possible in these areas for better monitoring.

4.1.3. Node Betweenness

After calculation, the betweenness values of each node were obtained, as shown in Table 2.

Table 2. Node betweenness.

Node Number	Betweenness	Node Number	Betweenness	Node Number	Betweenness
1	102.00	18	61.92	35	197.16
2	565.89	19	283.13	36	289.28
3	378.12	20	78.99	37	218.11
4	221.16	21	486.15	38	192.14
5	130.40	22	137.15	39	98.22
6	306.88	23	411.83	40	132.90
7	250.46	24	723.62	41	334.51
8	299.69	25	500.12	42	121.37
9	188.87	26	189.15	43	225.03
10	4.00	27	416.16	44	270.03
11	102.00	28	288.11	45	40.35
12	230.40	29	398.55	46	199.00
13	80.20	30	375.98	47	44.71
14	196.96	31	34.08	48	194.53
15	238.06	32	34.08	49	102.00
16	355.58	33	102.00		
17	62.16	34	396.83		

4.1.4. Node User Disaster Prevention Impact Factor Weight

The node water shortage rate, the node emergency support level score and the node betweenness value were used as the impact factor indicators. The parameters of each node and the relative influence value were calculated by Matlab software programming, and the relative influence value of each node is normalized. The weight values of the node impact factor are shown in Figure 7.

Figure 7 shows that the darker the node color, the higher the weight of the node impact factor, and the more important the node. The weight values of the node users' impact factor reflect the post-earthquake functional importance of the node. The nodes with relatively high impact factor weights were node 19, node 25, node 24, node 23, node 22, node 8, node 34 and node 41. These nodes are very crucial for the shelter of residents after an earthquake and the rescue of secondary disasters, which should be protected.

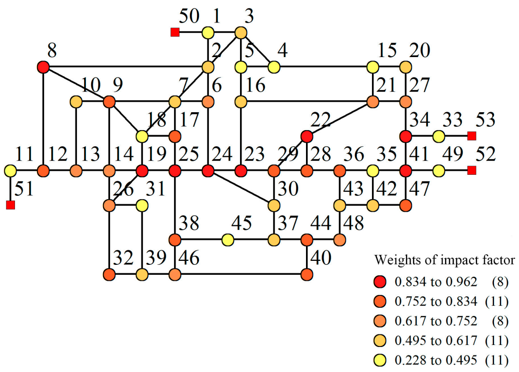

Figure 7. The ordering of node user impact factor weights.

4.2. Sensor Placement for Disaster Prevention in WDNs

4.2.1. Monitoring Domain Division Based on Three-Way Decision Cluster Integration

The K-means clustering method, fuzzy C-means clustering method, pedigree clustering method and dynamic classification method are common clustering methods for sensor placement. Each method has its own decision-making value. Based on the three-way decision cluster integration method, we integrated the K-means clustering method, fuzzy C-means clustering method, pedigree clustering method and dynamic classification method to divide the monitoring area of the WDN.

The three-way clustering integration method integrated four clustering methods to divide the monitoring domain of the WDN. As the three-way decision cluster integration method is not the focus of this article, the details can be found in [32]. The clustering results obtained by the K-means clustering method were taken as a reference to carry out cluster label matching, and the nodes that clearly belong to the corresponding category were divided into the positive domain of the corresponding category. After the voting matrix was constructed, the monitoring domain classification of the nodes was obtained according to the previous dividing rules, as shown in Tables 3 and 4. The nodes in the boundary domain belong to the boundary of the class, i.e., the nodes divided into the boundary domain can be effectively monitored by different monitoring points at the same time.

Table 3. Positive domain of three-branch clustering integration.

Category	Positive Domain								
1	42	47	24	30	43	48			
2	11	12	14	17	19	25			
3	49	23	28	29	33	34	35	36	41
4	10	26	31						
5	32	39							
6	15	20	21	22	27				
7	3	4	5	16	1	2			

Table 4. Boundary domain of three-branch clustering integration.

Category	Positive Domain					
1,5	37	38	40	44	45	46
2,4,5	7	8	9	13	18	
2,4,7	6					

The three-way decision integration clustering method integrates two-way decision clustering results into one three-way decision clustering result, which makes each category more uniform (Tables 3 and 4). When it is impossible to determine that an object belongs to a certain class of clusters, it is divided into boundary regions, indicating that the object may belong to multiple clusters, thus describing its fuzziness.

4.2.2. Sensor Placement for Disaster Prevention in WDNs for Important Users

According to the classification of the monitoring domain and the comprehensive sensitivity of nodes, the sensitivity threshold is set as 0.85, so that we obtain the sensor placement nodes, which are node 44, node 14, node 23, node 10, node 32, node 20 and node 6. MapInfo software was used to draw the final placement diagram, as shown in Figure 8.

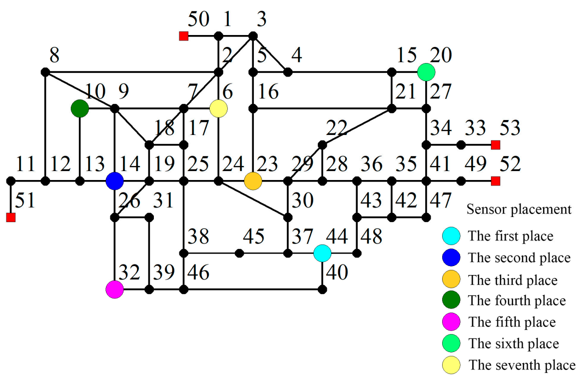

Figure 8. Sensor placement for disaster prevention in water distribution networks for important users.

4.3. Sensor Placement in WDNs Based on Traditional Models

In traditional sensor placement, clustering algorithms are usually used to classify monitoring points based on the sensitivity matrix. Clustering centers are used as monitoring points where sensors are placed and corresponding categories are monitoring areas. The sensitivity curves of some nodes are shown in Figure 9, and the pedigree clustering tree is shown in Figure 10. It should be noted that the fuzzifier parameter of the fuzzy C-means clustering method was 2, and the membership values are shown in Table 5. The membership degree of the dynamic classification method was determined by the entropy weight method.

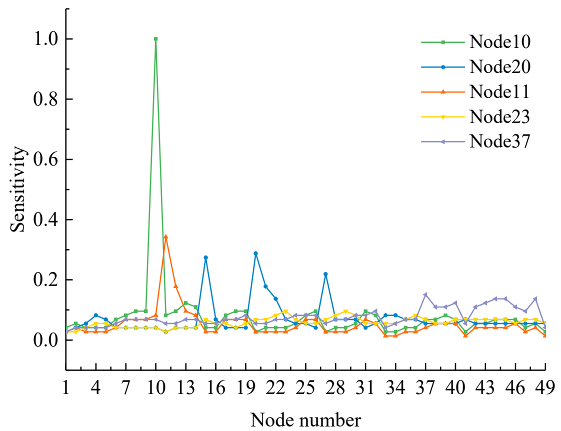

Figure 9. Sensitivity curves of some nodes.

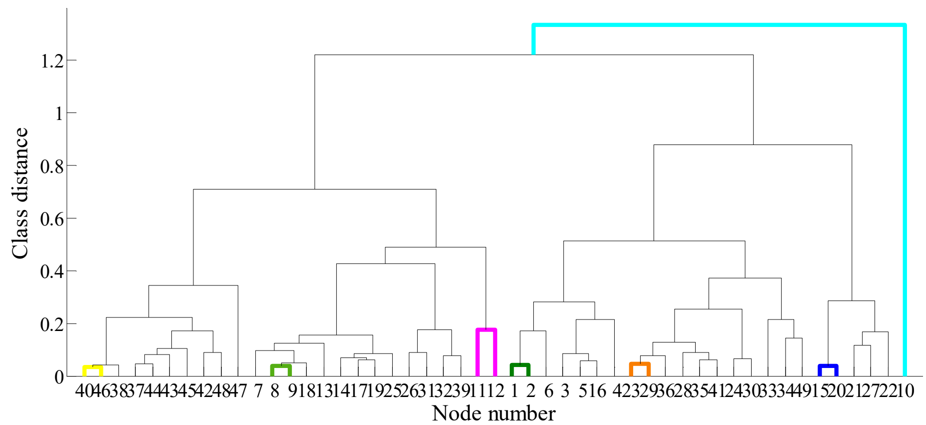

Figure 10. Pedigree clustering tree.

Table 5. Membership values.

Classification	N1	N2	N3	N4	N5	N6	N7	N8	N9	N10
1	0.118	0.116	0.030	0.172	0.068	0.106	0.042	0.015	0.011	0.132
2	0.029	0.027	0.006	0.082	0.014	0.024	0.012	0.005	0.003	0.116
3	0.044	0.046	0.009	0.077	0.019	0.065	0.051	0.018	0.015	0.146
4	0.101	0.111	0.018	0.112	0.035	0.281	0.486	0.824	0.850	0.163
5	0.091	0.096	0.022	0.135	0.046	0.149	0.088	0.027	0.022	0.145
6	0.072	0.077	0.014	0.098	0.028	0.154	0.266	0.090	0.082	0.161
7	0.545	0.527	0.902	0.324	0.791	0.221	0.054	0.021	0.016	0.136
Classification	**N11**	**N12**	**N13**	**N14**	**N15**	**N16**	**N17**	**N18**	**N19**	**N20**
1	0.117	0.084	0.038	0.021	0.028	0.138	0.027	0.016	0.013	0.015
2	0.062	0.036	0.015	0.008	0.876	0.031	0.009	0.005	0.004	0.934
3	0.114	0.094	0.061	0.043	0.017	0.033	0.054	0.021	0.030	0.009
4	0.232	0.332	0.475	0.374	0.017	0.056	0.311	0.776	0.147	0.009
5	0.140	0.119	0.070	0.047	0.023	0.083	0.071	0.031	0.034	0.012
6	0.189	0.223	0.296	0.483	0.017	0.046	0.497	0.130	0.756	0.009
7	0.146	0.112	0.045	0.024	0.023	0.613	0.031	0.022	0.015	0.012
Classification	**N21**	**N22**	**N23**	**N24**	**N25**	**N26**	**N27**	**N28**	**N29**	**N30**
1	0.159	0.219	0.527	0.067	0.022	0.047	0.029	0.659	0.464	0.066
2	0.436	0.248	0.026	0.013	0.007	0.019	0.886	0.018	0.029	0.009
3	0.059	0.080	0.047	0.079	0.070	0.164	0.014	0.031	0.058	0.050
4	0.065	0.086	0.046	0.072	0.126	0.172	0.014	0.038	0.051	0.036
5	0.102	0.146	0.215	0.629	0.070	0.106	0.021	0.124	0.256	0.758
6	0.064	0.084	0.047	0.095	0.683	0.445	0.014	0.036	0.054	0.046
7	0.115	0.138	0.091	0.045	0.022	0.047	0.021	0.095	0.087	0.034
Classification	**N31**	**N32**	**N33**	**N34**	**N35**	**N36**	**N37**	**N38**	**N39**	**N40**
1	0.058	0.058	0.292	0.503	0.771	0.772	0.047	0.023	0.056	0.019
2	0.028	0.027	0.097	0.058	0.014	0.015	0.016	0.009	0.027	0.007
3	0.218	0.342	0.088	0.052	0.023	0.025	0.639	0.758	0.444	0.799
4	0.173	0.133	0.099	0.062	0.027	0.025	0.052	0.043	0.106	0.035
5	0.121	0.126	0.150	0.119	0.071	0.091	0.132	0.066	0.123	0.057
6	0.347	0.262	0.096	0.058	0.025	0.025	0.082	0.082	0.197	0.068
7	0.056	0.053	0.179	0.150	0.069	0.047	0.032	0.019	0.048	0.016
Classification	**N41**	**N42**	**N43**	**N44**	**N45**	**N46**	**N47**	**N48**	**N49**	
1	0.821	0.136	0.074	0.048	0.042	0.026	0.187	0.089	0.373	
2	0.015	0.028	0.024	0.017	0.016	0.010	0.062	0.022	0.048	
3	0.019	0.243	0.486	0.631	0.650	0.742	0.177	0.381	0.060	
4	0.021	0.078	0.068	0.053	0.056	0.045	0.110	0.077	0.078	
5	0.054	0.343	0.200	0.136	0.112	0.070	0.222	0.264	0.129	
6	0.020	0.101	0.102	0.084	0.092	0.086	0.122	0.109	0.070	
7	0.050	0.071	0.046	0.032	0.030	0.021	0.119	0.059	0.242	

In this paper, we used eight methods for sensor placement in WDNs, and the sensor placements by the eight methods are shown in Table 6. In addition to the four clustering algorithms used before, the node correlation coefficient method, the effective independence method, the improved Fisher information matrix maximization criterion and the impact ranking method were also used. The idea of voting was used to integrate the monitoring information as well as to fuse the consistency of various algorithms. The node numbers in parentheses indicate the nodes strongly related to the front nodes, which can also be used as monitoring points for the sensor installation.

Table 6. Comparison of various methods.

Methods	Sensor Placements
K-means clustering [33]	48, 8, 41, 10, 32, 27, 3
Pedigree clustering	10, 15 (20), 23 (29), 1 (2), 11 (12), 8 (9), 40 (46)
Fuzzy C-means clustering	41 (36), 20 (27), 40 (38), 9 (8), 30 (24), 19 (25), 3 (5)
Dynamic classification	10, 40, 42, 8, 41, 5, 1
Node correlation coefficient method	10 (13), 11 (12), 15 (20), 47 (42), 33 (34), 4 (5), 31 (26)
Effective independence method	39 (32), 10, 15 (20), 13 (14), 22, 29 (23), 3 (5)
Improved Fisher information matrix maximization criteria [32]	10, 33, 4, 47, 11, 22, 15
Influence ranking method	10, 15, 20, 39, 31, 32, 45

Finally, based on the idea of voting, we carried out a statistical analysis of sensor placement nodes in Table 6, selected the top 10 nodes as the alternative monitoring nodes, and the placement on the basis of the division of monitoring areas is shown in Figure 11.

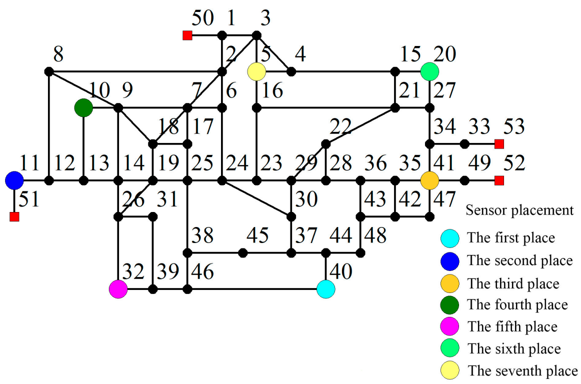

Figure 11. Sensor placement based on traditional models.

According to the hydraulic data of the WDN, it can be seen that pressure value of node 32 is the lowest, which is 19.32 m under the standard working condition, and the second lowest nodal pressure value is node 10, which is 20.13 m. The next lowest is node 41, for which the pressure value is 20.15 m. These three nodes are in a relatively low water pressure. The water demand of node 11 is the second lowest, at 97.2 m^3/h. Comparing the hydraulic information, we found that the nodes with lower pressure and water requirement are more sensitive to the changes of pressure and water requirement caused by leakage. The monitoring sensors should be placed at the end of pipework, which is more sensitive to pressure, as far as possible, which is consistent with that described in Jianwen Liang [31].

5. Discussion

The sensor placement of the two models is as follows:

1. Sensor placement based on traditional models: node 40, node 11, node 41, node 10, node 32, node 20 and node 5.
2. Sensor placement for disaster prevention in WDNs for important users: node 44, node 14, node 23, node 10, node 32, node 20 and node 6.

In terms of the node location, Figures 7 and 10 show that the sensors placed in node 40 and node 11 in the traditional model are close to node 44 and node 14, respectively, in the model presented herein. Node 10, node 32 and node 20 are selected as monitoring placements in both the two models. This means that the above three nodes are still suitable for monitoring the pressure changes of pipework as sensor placements, considering both sensitivity and node users' impact factors.

In terms of node importance, the monitoring points node 40, node 11, node 41 and node 5 in the traditional model become node 44, node 14, node 23 and node 5 in the model presented herein. From Figure 6, it can be seen that the sensor placements based on the model presented herein are located at or near the nodes with high impact factors, indicating that the placements are more important in post-earthquake emergency support, network topology and water shortage rate.

6. Conclusions

In this paper, the post-earthquake function importance and network importance of nodes are introduced into the placement of monitoring points to realize the layout of disaster prevention monitoring points in WDNs, with good compatibility with health monitoring layout. Three-way decision clustering methods are introduced to comprehensively consider the decision value of integrating multiple clustering methods, which can be used as a way to consider the influence of different factors in sensor placement. The work in this paper has formed a technical tool for sensor placement for disaster prevention, which is of great significance for urban post-earthquake emergencies.

Author Contributions: Conceptualization, J.W., W.W. and D.M.; methodology, J.W. and W.W.; software, J.W. and Z.H.; validation, J.W.; formal analysis, D.M.; investigation, J.W.; resources, D.M. and W.W.; data curation, J.W.; writing—original draft preparation, J.W.; writing—review and editing, J.W., D.M. and W.W.; visualization, J.W.; supervision, D.M.; project administration, W.W.; funding acquisition, W.W. All authors have read and agreed to the published version of the manuscript.

Funding: This research was funded by the National Natural Science Foundation of China (Grant No. 51678017), National Key R&D Program of China (Grant No. 2018YFD1100902-1), Research Project on Major Policy Theory and Practice of China Earthquake Administration (CEAZY2019JZ14), Key Project of Earthquake Engineering and Engineering Vibration Key Laboratory of China Earthquake Administration (2019EEEVL0501).

Conflicts of Interest: The authors declare no conflict of interest. The funders had no role in the design of the study; in the collection, analyses, or interpretation of data; in the writing of the manuscript, or in the decision to publish the results.

References

1. Liu, S.; Zhang, X. *Investigation Report on Earthquake Disaster and Relief of Water Supply System Based on Wenchuan Earthquake*; Tongji University Press: Shanghai, China, 2013; pp. 4–10. ISBN 978-7-5608-5060-3.
2. Li, J.; Liu, W.; Bao, Y.F. Genetic algorithm for seismic topology optimization of lifeline network systems. *Earthq. Eng. Struct. Dyn.* **2008**, *37*, 1295–1312. [CrossRef]
3. Zhang, C.; Lin, Z.Z.; Wen, F.S.; Ledwich, G.; Xue, Y.S. Two-stage power network reconfiguration strategy considering node importance and restored generation capacity. *IET Gener. Transm. Dis.* **2014**, *8*, 91–103. [CrossRef]
4. Fan, W.L.; Hu, P.; Liu, Z.G. Multi-attribute node importance evaluation method based on Gini-coefficient in complex power grids. *IET Gener. Transm. Dis.* **2016**, *10*, 2027–2034.
5. Wang, F.; Zheng, X.Z.; Chen, S.; Zhou, J.L. Emergency Repair Scope Partition of City Water Distribution Network: A Novel Approach Considering the Node Importance. *Water Resour. Manag.* **2017**, *31*, 3779–3794. [CrossRef]
6. Kermarrec, A.M.; Merrer, E.L.; Sericola, B.; Trédan, G. Second order centrality: Distributed assessment of nodes criticity in complex networks. *Comput. Commun.* **2011**, *34*, 619–628. [CrossRef]
7. Zareie, A.; Sheikhahmadi, A.; Jalili, M. Influential node ranking in social networks based on neighborhood diversity. *Future Gener. Comput. Syst.* **2019**, *94*, 120–129. [CrossRef]
8. Fragiadakis, M.; Christodoulou, S.E.; Vamvatsikos, D. Reliability Assessment of Urban Water Distribution Networks Under Seismic Loads. *Water Resour. Manag.* **2013**, *27*, 3739–3764. [CrossRef]

9. Cao, X.X.; Qie, Z.H.; Wang, W.Z.; Wu, X.M. Genetic optimization of flow monitoring points for water supply network fault diagnosis. *China Rural Water Hydropower* **2013**, *1*, 22.
10. Chen, L.L.; Zhuang, W.T.; He, X. Pressure monitoring point layout of water supply network based on information maximization criterio. *J. Shanghai Univ. Nat. Sci.* **2015**, *21*, 640–647.
11. Kowalski, D.; Kowalska, B.; Kwietniewski, M. Monitoring of water distribution system effectiveness using fractal geometry. *Bull. Polsh Acad. Sci. Tech.* **2015**, *63*, 155–161. [CrossRef]
12. Kirstein, J.K.; Albrechtsen, H.J.; Rygaard, M. Topological clustering as a tool for planning water quality monitoring in water distribution networks. *Water Sci. Tech. Water Supply* **2015**, *15*, 1433–1435. [CrossRef]
13. Nejjari, F.; Sarrate, R.; Blesa, J. Optimal pressure sensor placement in water distribution networks minimizing leak location uncertainty. *Procedia Eng.* **2015**, *119*, 953–962. [CrossRef]
14. Soldevila, A.; Blesa, J.; Tornil-Sin, S.; Fernandez-Canti, R.M.; Puig, V. Sensor placement for classifier-based leak localization in water distribution networks using hybrid feature selection. *Comput. Chem. Eng.* **2018**, *108*, 152–162. [CrossRef]
15. Cornell University. *GIRAFFE User's Manual Version 4.2*; Cornell University: Ithaca, NY, USA, 2008.
16. Shi, P.; O'rourke, T.D.; Wang, Y. Simulation of earthquake water supply performance. In Proceedings of the 8th National Conference on Earthquake Engineering, Oakland, CA, USA, 18–22 April 2006.
17. Shi, P.; O'rourke, T.D. Seismic Response Modeling of Water Supply Systems. Available online: http://www.eng.buffalo.edu/mceer-reports/08/08-0016.pdf (accessed on 13 April 2019).
18. Wang, Y.; O'rourke, T.D. *Seismic Performance Evaluation of Water Supply Systems*; Technical Report MCEER-08-0016; Multidisciplinary Center for Earthquake Engineering Research: Buffalo, NY, USA, 2006.
19. Laucelli, D.; Giustolisi, O. Vulnerability Assessment of Water Distribution Networks under Seismic Actions. *J. Water Resour. Plan. Manag.* **2015**, *141*, 04014082. [CrossRef]
20. Yoo, D.G.; Kang, D.S.; Kim, J.H. Seismic reliability assessment model of water supply networks. In *World Environmental and Water Resources Congress 2013: Showcasing the Future*; Patterson, C.L., Struck, S.D., Murray, D.J., Eds.; American Society of Civil Engineers: Reston, VA, USA, 2013; pp. 955–966.
21. Han, Z.; Ma, D.H.; Hou, B.W.; Wang, W. Post-earthquake hydraulic analyses of urban water supply network based on pressure drive demand model. *Sci. Sin. Technol.* **2019**, *49*, 351–362. [CrossRef]
22. Duda, R.; Hart, P.; Stork, D. *Pattern Classification*, 2nd ed.; John Wiley & Sons: New York, NY, USA, 2001.
23. Lingras, P.; Yan, R. Interval clustering using fuzzy and rough set theory. In *IEEE Annual Meeting of the Fuzzy Information*; IEEE: Piscataway, NJ, USA, 2004; pp. 780–784.
24. Hu, L.C.; Yu, H. A voting-based clustering method for three decision-making branches. *J. Chin. Comput. Syst.* **2016**, *37*, 1741–1745.
25. Wagner, J.M.; Shamir, U.; Marks, D.H. Water distribution reliability simulation methods. *J. Water Resour. Plan. Manag.* **1988**, *114*, 276–294. [CrossRef]
26. Jeon, S.S.; O'Rourke, T.D. Northridge earthquake effects on pipelines and residential buildings. *Bull. Seismol. Soc. Am.* **2005**, *95*, 294–318. [CrossRef]
27. GB/T 51327-2018. *Standard for Urban. Planning on Comprehensive Disaster Resistance and Prevention*; China Construction Industry Press: Beijing, China, 2018.
28. Wang, H.Y.; Huang, Q.; Li, C.T. *Graph. Theory Algorithm and Matlab Implementation*; Beijing University of Aeronautics and Astronautics Press: Beijing, China, 2010; ISBN 978-7-8112-4940-8.
29. Lin, Y.Y. *Design of Real-Time Monitoring System for Urban. Water Supply Network and Optimal Layout of Monitoring Points*; South China University of Technology: Guangzhou, China, 2013.
30. Wang, X.J.; Wangm, Z.Y. On the selection of pressure monitoring points in water supply network. *China Water Supply Drain.* **1989**, *5*, 9–12.
31. GB/T 17742-2008. *The Chinese Seismic Intensity Scale*; China Standard Press: Beijing, China, 2008.
32. Wu, J.J. *Study on Monitoring Placement of Urban. Water Supply Network Based on Disaster Prevention Function*; Beijing University of Technology: Beijing, China, 2019.
33. Jain, A.K. Data clustering: 50 years beyond K-means. *Pattern Recogn. Lett.* **2010**, *31*, 651–666. [CrossRef]